RSC Advances

ROYAL SOCIETY OF CHEMISTRY

www.rsc.org/advances

Journal Name

RSCPublishing

ARTICLE

Nanoengineered drug-releasing aluminium wire implants: Comparative investigation of nanopore geometry, drug release and osteoblast cell adhesion

Cite this: DOI: 10.1039/x0xx00000x

Received 00th January 2015,
Accepted 00th January 2015

DOI: 10.1039/x0xx00000x

www.rsc.org/

Shafiur Rahman [a], Renee Ormsby [b], Abel Santos [a], Gerald J. Atkins [b], David M. Findlay [b] and Dusan Losic [a]*

In this study, drug-releasing aluminium (Al) wire implants featuring nanoporous alumina (NPA) layers produced by different anodization approaches are systematically investigated as potential platforms for localized drug delivery and bone therapy. NPA-Al wires are fabricated by symmetric and asymmetric two-step anodization approaches in sulphuric and oxalic acid electrolytes. The top surface of resulting NPA layers display different geometric features and nanoporous structure. While a symmetric two-step anodization process yields nanoporous layers based on single nanopore cells, asymmetric anodization leads to a hierarchical nanoporous structure composed of 2-10 nanopores per cell, which can be precisely engineered by the anodization conditions. The drug-releasing performance of the resulting NPA layers is assessed through a series of *in vitro* studies. The results reveal that NPA-Al wire implants with hierarchical nanoporous structures present enhanced drug loading and release capabilities as compared to implants based on single nanopore cells. Biopolymer (chitosan) coating layers are incorporated onto these NPA-Al drug-loaded wire implants in order to control the release of drug over a longer time period. Finally, the potential osseointegration of NPA-Al implants is evaluated by osteoblast cell adhesion experiments. NPA-Al implants with a hierarchical nanopore structure show significantly greater osteoblast cell attachment as compared to NPA-Al wires produced by symmetric anodization and their chitosan coated forms. Overall, this study demonstrates that drug releasing NPA-Al wires implants with precisely engineered nanopore structures have great potential as implant platforms for treatment of localized diseases such as bone cancer and osteomyelitis.

Introduction

Local implantable drug delivery systems have drawn tremendous attention in recent years as a promising alternative to conventional systemic therapy, which presents some innate limitations such as poor bio-distribution, non-selectivity, toxicity, and unfavourable pharmacokinetics.[1] Their potential to directly deliver sufficient drug to the site of diseases and ability to provide a precise control over payload release makes local implantable drug delivery systems an attractive choice to treat different diseases in a local manner. In particular, these medical devices have been recently envisaged for treating bone diseases such as osteomyelitis and bone cancer.[2] Recent progress in better understanding of bone biology and its architecture, pathogenesis, and healing processes has contributed immensely to the development of various micro and nanotechnology based local delivery carriers and devices. These systems have the ability to deliver therapeutics to the injury site in difficult-to-access organs and to promote favourable cellular activity while preventing pathology.[3,4] So far, numerous biomaterials such as ceramic, fibre mat, acrylic polymer, poly (lactic-co-glycolic acid), collagen, hyaluronan, chitosan, fibrin, silk, hydroxyapatite and calcium phosphate cements have been explored as local drug delivery platforms.[5] Although many of these materials have been suggested to be suitable for clinical use, their poor reproducibility and large variation of porosity often cause undesirable initial burst drug release and uncontrollable release kinetics. Importantly, most of these materials lack the essential mechanical properties and rigidity required especially for load bearing applications into bone, leading to limited clinical utility as drug-releasing platforms for treating bone-related diseases.[6] Delivering therapeutics into the bone is difficult due to its complex porous architecture filled with abundant bone marrow and a high fat content.[6] It is also a major challenge to reach some difficult-to-access areas of bone. Therefore, to deliver therapeutics in a consistent manner to treat diseases such as cancer (e.g. osteosarcoma), infection and localised inflammation of bone remains challenging.[7]

To overcome these limitations, metal-based nanoengineered delivery devices have recently emerged as a promising alternative. These systems provide not only controllable drug delivery but also improved mechanical support, enhanced bioactivity and favourable tissue regeneration.[8–10] Among such approaches, nanoengineered titanium (Ti) with a layer of titania nanotubes (TNTs) generated by electrochemical anodization has been regarded as one of the most promising biomaterials for bone implants. TNTs-Ti implants are attractive due to their unique properties, including a highly ordered nanotubular structure, controllable dimensions, a high surface area and aspect ratio, considerable mechanical and chemical stability, biocompatibility and excellent osseointegration properties.[11–13] These nanoengineered TNTs-Ti materials have demonstrated their ability to act as drug releasing therapeutic implants in orthopaedics,[13]

dentistry[14] and brain,[15] with delivery of number of drugs for bone therapy including antibiotics, anti-inflammatories, anticancer agents and growth factors.[16] However, although extensive research has been accomplished on TNTs as planar implant devices and these appear to be inconvenient for insertion into bone, these implantable devices require a large degree of surgical intervention.[3] To overcome this limitation, a minimally invasive needle puncturing approach based on nanoengineered Ti wire as a bone implant has been recently developed by our group.[17] These wire implants can be conveniently inserted into bones, including narrow areas within the bone, which makes it possible to achieve difficult-to-access areas with minimal surgery. Unlike planar devices with one-sided nanoengineered pores or tubes, these cylindrical wire devices are able to release payloads multi-directionally and homogeneously into the surrounding tissue.[17]

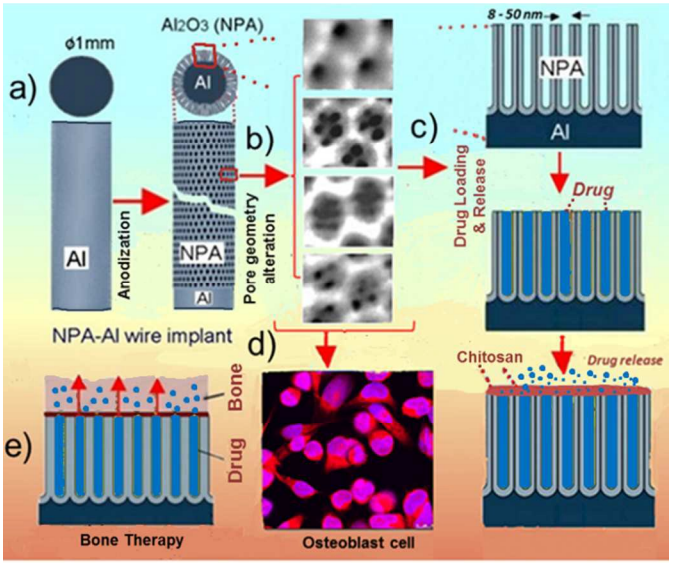

Fig. 1 Nanoporous alumina-aluminium wire implants for localized therapy. a-b) Scheme of Al wire implants preparation and alteration of pore geometry by anodization, c) drug loading, chitosan coating and *in vitro* drug release, d) relative osteoblast cell adhesion, and e) their potential application in bone therapy.

In addition to TNTs-Ti, electrochemically engineered nanoporous alumina (NPA) generated on the surface of aluminium (Al) substrates has also attracted attention for localized drug delivery applications, which have already shown their potential to be used as orthopaedic,[18–24] dental[25,26] and coronary stent implants.[27–29] The major advantages of NPA over TNTs include better mechanical stability and rigidity of the porous layer and controllable engineering of pore nanostructure dimensions and geometry by an electrochemical anodization process.[8] Typically, NPA is produced by a two-step anodization process conducted at a constant voltage in both steps (i.e. symmetric anodization) using acid electrolytes such as aqueous solutions of oxalic and sulphuric acid.[30-32] The result is a layer of NPA featuring cylindrical nanopores hexagonally distributed across the surface of the oxide film with single nanopore cells. The two-step anodization process is typically performed under symmetric conditions, where the anodization parameters (e.g. anodizing voltage, type and concentration of the acid electrolyte, etc.) are the same in both steps. In an asymmetric two-step anodization process, however, the anodization conditions of each step are different. Under certain conditions, this electrochemical approach yields the production of another type of NPA structure, so-called hierarchical NPAs. These NPA films consist of an outer hexagonal lattice of hemispherical concavities inside which small pores grow. The architectural characteristics of the outer concavities and the inner nanopores depend on the anodization conditions used during the first and second anodization steps, respectively.[33,34] Up until now, anodic films based on NPA have been demonstrated as a platform for drug delivery applications using planar Al substrates.[23–29] As a suitable alternative platform for bone therapy Al wire has been recently demonstrated a potential local therapeutic implant.[35,36] However, the challenge still lies in their appliactions as implants for localized bone applications to improve the properties of their electrochemically engineered surfaces that promotes bone cell attachment and osseointegration together with appropriate drug-releasing abilities for clinical therapy.

Thus, the first aim of our study was to demonstrate new nanofabrication approaches towards designing an advanced drug-releasing NPA-Al wire implant with improved nanoporous structure and topography for combinatorial drug delivery and osseointegration. Two types of NPA-Al wires were prepared with a single nanopore cells and hierarchical by symmetric and asymmetric using two-step anodization approaches in order to explore their drug-loading/releasing and bone cell integration properties. Then, our specific aims were to demonstrate the influence of the nanopore geometry and nanotopography of NPA-Al implants on the loading, *in vitro* drug release and bone cell (osteoblast) attachment. NPA wire implants prepared with different nanopore topography under specific anodization conditions were explored using indomethacin as a model drug including several strategies to extend drug release.

Experimental

Materials

High purity (99.997%) Al wires, 1 mm diameter, supplied by Alfa Aesar (USA) were used as the substrate material. A model anti-inflammatory drug, indomethacin, was used in this study and was purchased from Sigma-Aldrich, Australia. Oxalic acid ($C_2H_2O_4$), sulphuric acid (H_2SO_4), phosphoric acid (H_3PO_4), perchloric acid ($HClO_4$), chromium trioxide (CrO_3), nitric acid (HNO_3) hydrochloric acid (HCl) and cupric chloride ($CuCl_2$) were purchased from Sigma-Aldrich (Australia) and used as received. Ultrapure water Option Q–Pure labs (Australia) was used for preparing all the solutions used in this study.

Nanofabrication of NPA-Al wire implants

Al wires were cut into 10 cm long pieces, cleaned by sonication for 30 min in water and acetone and air dried. Electrochemical polishing of cleaned wires was performed by cold mixture of perchloric acid and ethanol (v:v, 1:4) at a constant voltage of 20 V for 1 min to obtain wires with mirror-like smooth surface. This process was performed in a custom-designed electrochemical cell consisting of a stainless steel wire as a counter electrode. The wires were then cleaned with water, air dried and partially protected with a pipette tip to expose only 9 mm length of electropolished wire for two-step electrochemical anodization using 0.3 M oxalic and 0.3 M sulphuric acid electrolytes.[30,31] As mentioned above, two electrochemical approaches, symmetric and asymmetric, were used in this study. At first, we conducted a first anodization step with the wires in oxalic acid at constant voltage of 40 V and in sulphuric acid at 25 V for 6 h at 5°C both. The anodized wires were then chemically treated using a mixture of 0.2 M chromic acid and 0.4 M phosphoric acid at 70 °C for 3 h to remove the resulting anodic film with disorganised nanopores on its top, cleaned and air dried. For symmetric process,

the resulting wires were treated in the second anodization step using oxalic acid at constant voltage of 40 V and sulphuric acid at 25 V for 1-10 h to prepare symmetric NPA-Al wire implants labelled as NPA-$Al_{(Sym(40-40)-Ox)}$ and NPA-$Al_{(Sym(25-25)-Sulp)}$, respectively. However, for the asymmetric process, the second anodization step was conducted at voltages of 10, 20, and 55 V in oxalic acid and at 10, 15, and 20 V in sulphuric acid for 6 h to prepare asymmetric NPA-Al wire implants referred as to NPA-$Al_{(Asym(40-10/20/55)-Ox)}$ and NPA-$Al_{(Asym(25-10/15/20)-Sulp)}$, respectively. Based on the pore geometry and pore length growth rate with each type of implants, symmetric implants NPA-$Al_{(Sym(40-40)-Ox)}$ and NPA-$Al_{(Sym(25-25)-Sulp)}$ and asymmetric implants NPA-$Al_{(Asym(40-10)-Ox)}$ and NPA-$Al_{(Asym(25-10)-Sulp)}$ of similar pore length (20 μm) used for drug release and cell adhesion studies. Note that all of the prepared wires were cleaned, air dried and stored for future use just after anodization.

Structural characterization

Prepared NPA-Al wires were imaged initially by light microscopy. In order to facilitate viewing and confirm their morphological features, NPA-Al wires were cut into small pieces and Al was chemically removed from the middle of the wire piece using a mixture of HCl (10% w/w) and 0.1M $CuCl_2$ solution to expose the cylindrical NPA layer. Structural characterization of the wires before drug loading and after chitosan coating was carried out by SEM. All of the wire samples were mounted on a SEM sample holder using double-sided conductive carbon tape and coated with a 3–5 nm thick layer of platinum. Images, with a range of scan sizes at normal and at a 30° angle incidence, were acquired from the top and bottom surfaces, and cross-sectionally. Pore length growth, pore diameter and interpore distance of NPA-Al wires prepared by both processes were established using a field emission gun scanning electron microscope (FEG-SEM) (Quanta 450, Eindhoven, The Netherlands).

Drug loading into NPA-Al wire implants and chitosan coating

Indomethacin used as a model drug was dissolved in ethanol (50 mg/ml) and loaded into the NPA-$Al_{(Asym(40-10)-Ox)}$, NPA-$Al_{(Sym(40-40)-Ox)}$, NPA-$Al_{(Asym(25-10)-Sulp)}$ and NPA-$Al_{(Sym(25-25)-Sulp)}$ wires of 20 μm pore length using a method following immersion and drying technique.[17] In brief, all types of wires were fully immersed in the drug solution in a glass vial, sonicated for 5 min and then left standing on a vibration-free surface for 2 h, with very gentle shaking at 30 min intervals to promote loading inside the nanopores. The wires were then air-dried and excess drug was removed from the surface using phosphate buffered saline (PBS, pH 7.4) wetted soft tissue. Drug loaded NPA-$Al_{(Sym(40-40)-Ox)}$ and NPA-$Al_{(Sym(25-25)-Sulp)}$ wires were also coated using a polymer solution of chitosan (1% (w/v), chitosan + 0.8 vol.% acetic acid in ultra-pure water) by a single dip-coating process,[37] where wires were quickly dipped into solution, removed, and dried in an oven at 60 °C for 5 min.

***In vitro* drug release of NPA-Al wire implants**

For *in vitro* release studies, drug-loaded NPA-$Al_{(Asym(40-10)-Ox)}$, NPA-$Al_{(Sym(40-40)-Ox)}$, NPA-$Al_{(Sym(40-40)-Ox)}$+chitosan, NPA-$Al_{(Asym(25-10)-Sulp)}$, NPA-$Al_{(Sym(25-25)-Sulp)}$ and NPA-$Al_{(Sym(25-25)-Sulp)}$+chitosan were immersed separately in PBS (5 ml; pH 7.4) at room temperature using a procedure described previously.[15] In brief, 4 ml aliquots of buffer solution were removed and analyzed every 30 min up to the first 6 h and then once daily until 7 days. A representative sample of polymer coated wires were taken out of the solution, carefully dried in the oven at 60 °C for 5 min and examined using SEM to assess the degradation process of the polymer coating. After that, wires were replaced in 10 ml fresh PBS and sonicated for 5 h to extract unreleased drug. The aliquots were placed in a quartz cuvette and the concentration of released indomethacin was measured at 551 nm using a UV-visible spectrometer.

Relative osteoblast-like cell attachment and spread ability with NPA-Al wire implants

The human osteosarcoma cell line, HOS (American Type Culture Collection, Rockville, MD, USA), was used to investigate biocompatibility and cell adhesion and spreading across the surface of NPA-Al wire implants. Cells were cultured in α-modified minimal essential medium (Gibco) supplemented with ascorbate 2-phosphate (100 μM; Gibco), fetal calf serum (FCS, 5 vol. %; Sigma) and 1% penicillin (Sigma) at 37°C in 5% CO_2. NPA-Al wire implants {NPA-$Al_{(Sym(40-40)-Ox)}$, NPA-$Al_{(Asym(40-10)-Ox)}$, NPA-$Al_{(Sym(25-25)-Sulp)}$, NPA-$Al_{(Asym(25-10)-Sulp)}$, NPA-$Al_{(Sym(40-40)-Ox)}$+chitosan and NPA-$Al_{(Sym(25-25)-Sulp)}$+chitosan} and Al wires, used as test groups along with uncoated culture plastic as one of the controls, were gas sterilized and then placed in cell culture plates. Cells were removed from culture flasks using dispase and re-suspended at 1×10^6 cells/ml. For biocompatibility, an aliquot (50,000 cells) was added to each well of 48-well cell culture plates (Nunc) already containing test samples and the plates were incubated for 3 and 6 h at 37°C. Cell growth and viability was assessed using the crystal violet staining method, as described previously.[38] In brief, the medium was removed from the cells, which were rinsed gently with PBS and fixed using 10 % buffered formalin for 5–10 min, and washed again with PBS. The samples were then stained with 2–3 drops of 1 % (w/v) crystal violet for 20 min and excess stain was removed by washing in tap water. The cell-associated stain was then extracted with acetic acid (10 vol. %) for 20 min and then absorbance was measured at 570 nm by a spectrometry based plate reader.

For spread ability, an aliquot (25,000 cells) was added to each well of micro 8-well cell culture plates (Nunc) that already contained test samples and the plates were incubated for 3 and 6 h at 37°C. Cell spreading was observed using confocal microscopy imaging, as described elsewhere.[39] Briefly, after incubation the medium was removed from the cells, which were washed twice with PBS, fixed using 4% (w/v) paraformaldehyde/PBS for 10 min and rinsed in PBS, before being permeabilized in buffer containing 0.1 % (w/v) saponin (Sigma, Australia) for 30 min. Cells were washed twice in PBS, treated with phalloidin- tetramethyl rhodamine isothiocyanate (20 vol. % in PBS; Sigma) for 60 min in the dark at room temperature and then washed twice with PBS. To visualize nuclei, three drops of 40,6-diamidino-2-phenyindole (DAPI; Sigma) was added to each well and the samples were incubated in the dark for 60 min at room temperature, rinsed twice in PBS and immersed with PBS. Cell morphology was then visualized using confocal microscopy (Nikon C1-Z Confocal Microscope).

Statistical analysis

Student *t*-test and two-way analysis of variance followed by Tukey's multiple comparison test were used in this study. A value for $^{*}p< 0.05$ and $^{**}p< 0.01$ were considered significant.

Results and discussion

NPA-Al wire implants by symmetric two-step anodization using sulphuric and oxalic acid

NPA-Al wire implants featuring single nanopore cells were produced by symmetric two-step anodization process using either sulphuric or oxalic acid at constant voltage. The general structures of NPA-Al wires prepared by sulphuric acid based-anodization at constant voltage of 25 V and characterized using SEM imaging are presented in Fig. 2.

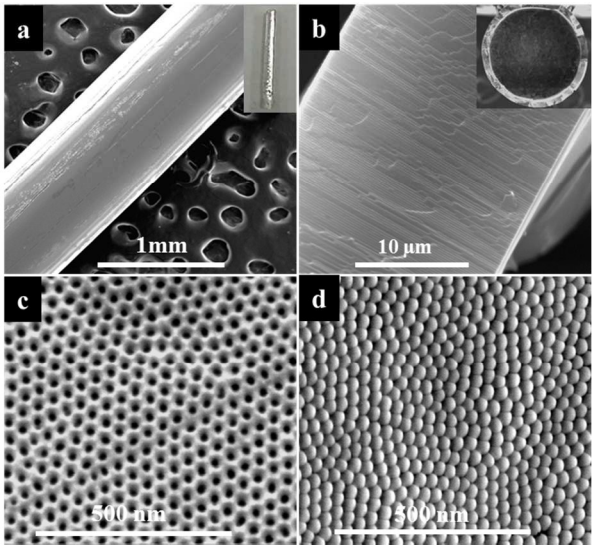

Fig. 2 NPA-Al wire implants (NPA-Al$_{(sym(25-25)-Sulp)}$) prepared by two-step symmetric anodization process at constant voltage of 25 V in sulphuric acid. SEM images of the implants with a) low resolution image showing a portion of wire (whole implant in inset, length 10 mm), b) a cross-section view of NPA layer showing nanopore length growth and cross-sectional view of wire after removal of Al showing cylindrical NPA layer around the wire, c) the top surface of NPA showing nanopore structures and d) the bottom surfaces showing closed ends of the nanopores (Al is removed for imaging purpose).

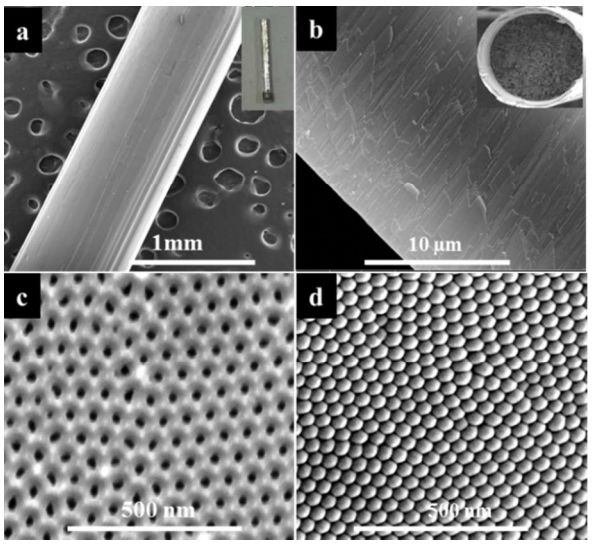

Fig. 3 NPA-Al wire implants (NPA-Al$_{(sym(40-40)-Ox)}$) prepared by two-step symmetric anodization process at constant voltage of 40 V in oxalic acid. SEM images of the implants with a) low resolution image showing a portion of wire (whole implant in inset, length 10 mm), b) a cross-section view of NPA layer showing nanopore length growth and cross-sectional view of wire after removal of Al showing cylindrical NPA layer around the wire, c) the top surface of NPA showing nanopore structures and d) the bottom surfaces showing closed ends of the nanopores (Al is removed for imaging purpose).

The figure shows a series of top (c), bottom (d) and cross-section images (b), which reveal that nanopores are arranged vertically aligned in a hexagonal fashion across the oxide layer on the Al surface of the implants. Digital images of the prepared wire implant revealed a characteristic shiny and smooth surface texture and a remarkably stable oxide layer deemed suitable for handling, which is a property desired for bone implants (Fig. 2a, inset). A high magnification SEM image confirmed growth of a NPA layer on the curved surface of Al wire. NPA layer shows some long vertical cracks (3–8 µm wide) across the entire wire with inter-distance about 80–100 µm. These cracks are caused by the mechanical stress produced by the volume expansion of oxide-metal and radial growth of NPA across the wire length.[30–35] Cross-sectional SEM images show the radial growth of densely packed NPA layer with homogeneous thickness or pore length and uniform cylindrical nanopores aligned parallel to each other (Fig.2b). High magnification SEM images of the top and bottom surfaces showed nanopores featuring diameters of 27.5±2.5 nm with closed ends at the bottom of the nanopores (Fig. 2c–d).

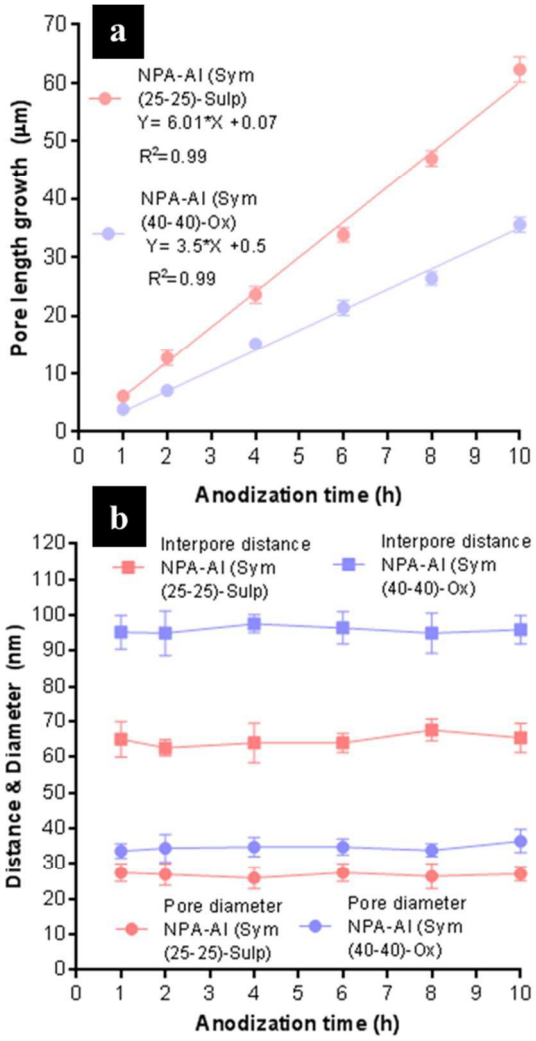

Fig. 4 Relationship between anodization time, and a) pore length (thickness of NPA layer) growth and b) pore diameters as well as inter-pore distance of NPA-Al wire implants. NPA-Al wire implants were prepared for 1-10 h by two-step symmetric anodization process in oxalic and sulphuric acid at constant voltage of 25 V and 40 V. Data represent mean ± st.dev. from at least 3 samples.

The general structures of NPA-Al wires prepared by oxalic acid at constant voltage of 40 V and characterized using SEM imaging are presented in Fig. 3. The figure shows a series of images from the top, bottom and cross-sections. Both digital and SEM images revealed that the structural morphology of the NPA-Al wires were similar to NPA-Al wire prepared by sulphuric acid regarding surface texture, growth of NPA layer on the Al wire, long vertical cracks, densely packed NPA with uniform and parallel channels and uniform closed nanopores bottom (Fig. 3a and inset). However, high magnification SEM images of the top surface reveal that nanopores produced in oxalic acid feature slightly bigger pore diameters of 35±3.5 nm (Fig. 3c–d), which is in good agreement with previous reports.[35]

It is worthwhile to mention that NPA layers on the wire surfaces generally present an amorphous phase of alumina similar to NPA layers formed on planar surface and their chemical composition is dependent on the acid electrolyte (i.e. oxalic and sulphuric) used for anodization.[36] These layers are robust, with a strong adherence to the underlying aluminium wire and do not get detached during regular handling and mechanical stresses.

To precisely prepare the NPA-Al wires with different pore length we established the dependence of pore length growth with anodization time from 1–10 h and determined the pore growth rate using both oxalic and sulphuric acid-based processes at the constant voltage of 40 V and 25 V. Furthermore, we determined the possible influence on pore diameter and interpore distance during different anodization times for NPA produced on wire substrates. The relationships obtained between anodization time and pore length growth, pore diameter and interpore distance are presented in Fig. 4. It was seen that pore length or thickness grows, as expected, almost linearly with time, showing a growth rate of approximately 3.5 μm h^{-1} and 6.1 μm h^{-1} for NPA produced in oxalic and sulphuric acid, respectively (Fig. 4a). This rapid formation of NPA layer using sulphuric acid is in good agreement with previous studies using planar Al substrates.[30,31] With the different anodization times, it was found that pore diameter and interpore distance remained almost constant at around 32-40 nm and 90-100 nm for oxalic acid-based process and 25-30 nm and 60-70 nm for sulphuric acid-based process (Fig. 4b), respectively. The lower interpore distance observed with NPA-Al wires prepared using sulphuric acid indicated higher pore density (more pores per square centimetre) compared to NPA-Al wires prepared in oxalic acid, which is in agreement with reported studies.[41-43] The results indicate that with changes of anodization time NPA-Al wires with desired pore layer thickness can be prepared and it does not affect their consistent small pore diameter as well as interpore distance. Overall, these investigations revealed that, using both sulphuric and oxalic acid-based symmetric anodization processes, NPA-Al wires with pore layers and small pore diameter can be prepared and both processes are effective with good reproducibility.

NPA-Al wire implants with altered pore geometry by asymmetric two-step anodization using sulphuric and oxalic acid

To alter pore geometry of the NPA-Al wires, we investigated the influence of variable anodization voltage in the final second step of the two-step anodization process using both sulphuric and oxalic acid. In this case, pore initiation sites are created primarily by anodization (first step) of Al wires either at 25 V using sulphuric acid or at 40 V using oxalic acid to form oxide layer as well as pores on the surfaces, which were subsequently removed to pattern the surface of Al wires with hexagonally arranged initiation sites. Pore initiation sites clearly indicated areas for single cell (data not shown) and this is already established in the literature.[44] Altered pore structures of NPA-Al wires prepared at 10, 15, and 20 V using sulphuric acid from Al wires, which were primarily anodized at 25 V in the first step and SEM images of the resulting nanoporous hierarchical structures are presented in Fig. 5. It was observed that an anodization voltage of 10 V and 15 V produced 3-6 very small pores of 10-15 nm and 2-4 pores of 10-12 nm, respectively, within a cell. However, those structures produced at 20 and 25 V showed a single nanopore per cell.

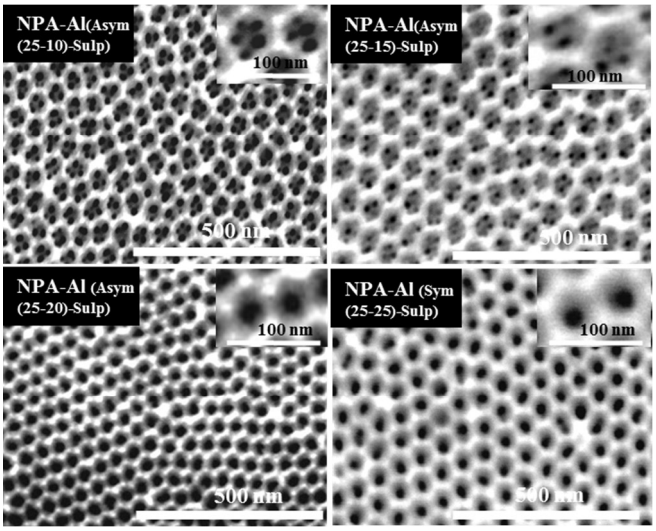

Fig. 5 Altered pore geometry of NPA-Al wire implants ($NPA\text{-}Al_{(Asym(25\text{-}10/15/20)\text{-}Sulp)}$ prepared by asymmetric anodization in sulphuric acid. SEM images of the top surface showing nanopores of the implants finally prepared at constant voltage of 10, 15, 20 and 25 V for 6 h in the second step of two-step anodization process. NPA-Al wire implants were prepared (in the first step) at a constant voltage of 25 V and then prepared for the second step by removing the oxide layer and pores formed on the surfaces.

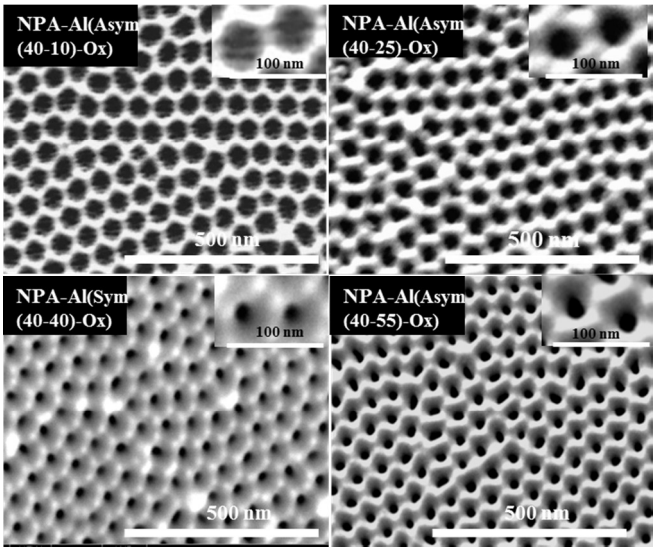

Fig. 6 Altered pore geometry of NPA-Al wire implants ($NPA\text{-}Al_{(Asym(40\text{-}10/25/55)\text{-}Ox)}$ prepared by asymmetric anodization in oxalic acid. SEM images of the top surface showing nanopores of the implants finally prepared at constant voltage of 10, 25, 40 and 55 V for 6 h in the second of the two-step anodization process. NPA-Al wire implants were prepared (in the first step) at a constant voltage of 40 V and then further processed for the second step by removing the oxide layer and pores formed on the surfaces.

Altered pore structures of NPA-Al wires prepared at 10, 25, and 55 V using oxalic acid from Al wires, which were primarily anodized at

40 V in the first step prior to removal of the oxide layer as well as pores formed on the surfaces, and observed using SEM are presented in Fig. 6. It was seen that that an anodization voltage of 10 V produced 3-7 very small pores of 7-11 nm within a cell as compared to 25, 40 and 55 V used, showing a single pore in a cell. These results indicate that pre-designed primary pore initiation sites, as well as the cell structure of NPA prepared at a constant anodization voltage, could be readily tuned and altered using an asymmetric two-step anodization approach. This altered anodization approach to fabricate NPA-Al wire implants with modified pores or surface appeared to be simple, robust and effective.

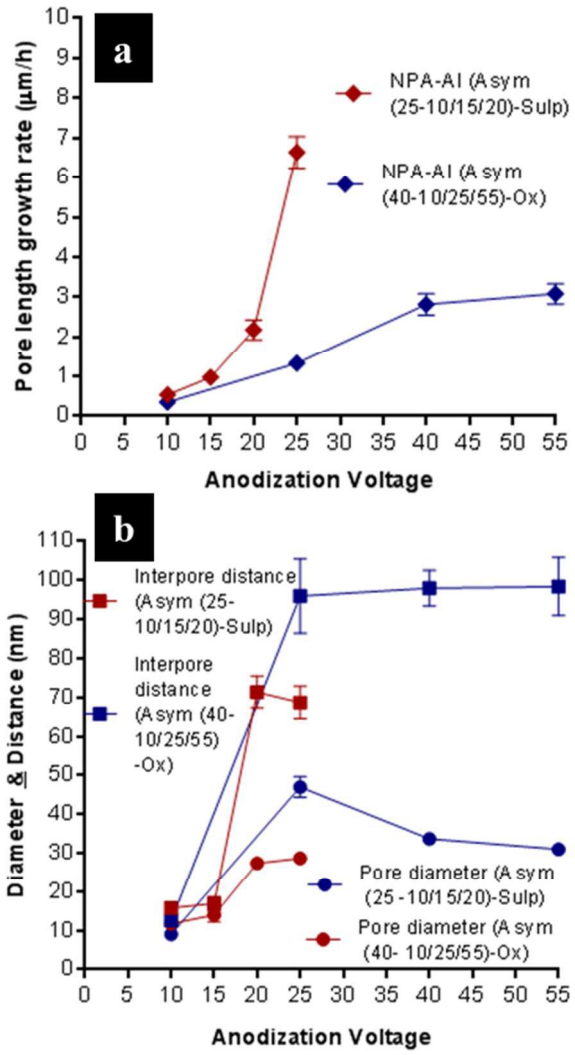

Fig. 7 Relationships between altered anodization voltage and a) pore length (thickness) growth and b) pore diameter as well as interpore distance of NPA-Al wire implants prepared by asymmetric anodization. NPA-Al wire implants were prepared in oxalic at constant voltage of 10, 25, 40 and 55 V and sulphuric acid at constant voltage of 10, 15, 20 and 25 V in the final second step of the two-step anodization process. NPA-Al wire implants were preliminarily (in first step) prepared at constant voltage of 40 V in oxalic and 25V in sulphuric acid, which were further processed for the second step by removing the oxide layer as well as pores formed on the surfaces. Data represent means ± st.dev. from at least 3 samples.

We also determined pore length growth and checked possible influences of the different anodization voltages on pore diameter and interpore distance for both processes using sulphuric and oxalic acid. The relationship between anodization voltage and pore length growth, pore diameter and interpore distance for both processes is presented in Fig. 7. With sulphuric acid, it was seen that pore length or thickness grows with changes of voltages, as expected, with a highest growth rate of 6.5 µm h^{-1} observed at 25 V (Fig. 3a). This increase of pore length with increase of anodization voltage is in agreement with many reported studies.[44] At low anodization voltages of 10 V and 15 V, pore diameter and interpore distance were found to be smaller within 9-16 nm and 12-18 nm ranges, compared to high anodization voltages of 20 V and 25 V, which resulted in relatively larger pore diameters of 25-30 nm and 65-75 nm (Fig. 7b). Using oxalic acid, pore length also grows with voltage, achieving the fastest growth rates at 40 V and 55 V (i.e. around 3.2 µm h^{-1} compared to lower voltages of 10 V and 25 V). The smallest pore diameter of 7-9 nm as well as interpore distance of 10-12 nm was found at 10 V compared to 25, 40 and 55 V showing pore diameter of larger than 30 nm as well as 85-105 nm of interpore distance. Overall, these results indicate that NPA-Al wires with various pore diameter and altered pore geometry can be prepared by an asymmetric two-step anodization approach using both sulphuric and oxalic acid. This altered approach could be valuable to increase the porosity of NPA-Al wire implant similar to pore-widening approach widely used to alter the pore geometry of NPA.[37]

In order to investigate the influence of altered pore structure on drug loading capacity, as well as on controlling the drug release characteristics, we prepared four types of NPA-Al wire implants with a constant pore length of 20 µm using both sulphuric and oxalic acid through both symmetric and asymmetric two-step anodization approach. Firstly, NPA-Al wires at 10 V for small pore (NPA-Al $_{(Asym(25-10)-Sulp)}$ and at 25 V for relatively large pore (NPA-$Al_{(Sym(25-25)-Sulp)}$ using sulphuric acid and secondly NPA-Al wires at 10 V for small pore (NPA-$Al_{(Asym(40-10)-Ox)}$ and 40 V for large pore (NPA-Al $_{(Sym(40-40)-Ox)}$ were prepared based on their individual pore length growth dependence with anodization time.

Drug loading and *in vitro* drug release characteristics

The gentle agitation step of drug loading approach allows infiltration of drug molecules inside the nanopore structure by removing trapped air bubbles and subsequent air-drying and removal of excess adsorbed drug from the wire surfaces ensures that molecules were only inside the nanopores. Table 1 summarises the drug loading results for the different types NPA-Al wires assessed in this study. The implants from both oxalic and sulphuric acid group with smaller pore diameter showed higher amounts of drug loading as compared to implants with large pore diameter. This increase in loading could be due to presence of a number of small pores within a cell, leading to soaking as well as retention of more drug molecules compared to single large pore within a cell. These results showed that by increasing the pore number, drug loading could be improved to meet disease specific dose requirement. Moreover, NPA-Al wires with further improved or precisely controlled drug loading could be easily achieved by using various other technique, including vacuum assisted infiltration as we described in previous studies,[8,14] and controlling loading conditions such as concentration of drug loading solution.

In vitro drug release kinetics investigated for six types of NPA-Al wire implant (including chitosan coated) are presented in Fig. 8, and Table 1. Cumulative release graphs showed a similar trend for all six types of implant and the trend could be considered as consisting of two phases. The first phase shows an initial sharp increase or burst release during the first 6 h, followed by the second stage with a slow and steady release over 7 days of measurement.

Table 1. Summary of drug loading and *in vitro* drug release characteristics of NPA-Al wire implants at constant pore layer thickness of 20 µm. Loading and release data represent means ± st.dev. from at least 3 samples.

Implants	Pore geometry within a single cell	Drug loading (µg)	Drug release in 6 h (%)	Drug release in 7 days (%)
NPA-Al *Asym(25-10)-Sulp*	PN: 3-6 PD:10-14 nm	43±1.2	43±0.9	81±1.1
NPA-Al *Sym(25-25)-Sulp*	PN: 1 PD: 27 nm	33±1.7	33±1.3	62±1.4
NPA-Al *Sym(25-25)-Sulp +Ch*	PN: 1 PD: 27 nm	33±1.7	23±1.4	52±1.6
NPA-Al *Asym(40-10)-Ox*	PN: 5-7 PD: 8-10 nm	41±1.1	45±2.3	84±1.8
NPA-Al *Sym(40-40)-Ox*	PN: 1 PD: 35 nm	32±1.6	35±2.1	70±1.3
NPA-Al *Sym(40-40)-Ox +Ch*	PN: 1 PD: 35 nm	32±1.6	22±1.2	54±2.1

PN: Pore number; PD: Pore diameter; Ch: Chitosan

The initial cumulative burst denoted by the straight portion of the curve could be regarded as a first-order release and be attributed to the fast diffusion of the drug molecules physisorbed on the top and upper parts of the nanopores. The slow and gradually increasing release with the second cumulative phase by all six types of implant could be due to diffusion of drug from the deep of the nanopore structures. The pattern can be considered zero-order release based on the Fickian diffusion law when drug release rate decreases as a function of time due to a reduction in concentration gradient.[29] In the first 6 h, it was seen that implants {(NPA-$Al_{(Asym(25-10)-Sulp)}$) and (NPA-$Al_{(Asym(40-10)-Ox)}$)} with multiple small pores of 8-14 nm within a cell showed higher burst drug release of 40-43% compared to implants {(NPA-$Al_{(Sym(25-25)-Sulp)}$) and (NPA-$Al_{(Sym(40-40)-Ox)}$)} with large single pores within a cell showing release of 30-35% of the drug molecule. After 7 days of measurement small pore containing implants also showed a higher cumulative release of 80-85% in comparison to implants with large single pores releasing 60-70% of the drug. This increased release of drug by multiple small pores could be attributed to their increased collective pore diameter or surface area, which accelerates the release of loaded drug from the nanopores. Implants (NPA-$Al_{(Sym(40-40)-Ox)}$) from the oxalic acid group with large pore diameter of 35 nm showed a small difference in drug release compared to implants (NPA-$Al_{(Sym(25-25)-Sulp)}$) of 27 nm pore diameter from the sulphuric acid group. All of the implants used in this study showed considerably low and sustained release up until 7 days of observation. The results indicate a considerable influence of the density or number of pore, as well as diameter on the drug release. These results are in agreement with pervious work on TNTs and NPA on planar substrates but the influence in drug release was less significant. The explanation is that in our study nanopores grown on curved surfaces feature smaller diameters (8-35 nm) compared with previous work where large pore diameters 50–150 nm were used[14,16]

In order to further control the drug release a thin chitosan layer was coated on the implants {(NPA-$Al_{(Sym(25-25)-Sulp)}$) and (NPA-$Al_{(Sym(40-40)-Ox)}$)} and investigated for its influence on drug release. Chitosan is already an approved polymer for local drug delivery applications as well as bone applications due to its various suitable properties, such as antibacterial and osseointegration.[37,38] SEM observation of the coating after formation on the implants and after 7 days of drug release confirmed the complete covering of the pores and gradual degradation respectively (data not shown).

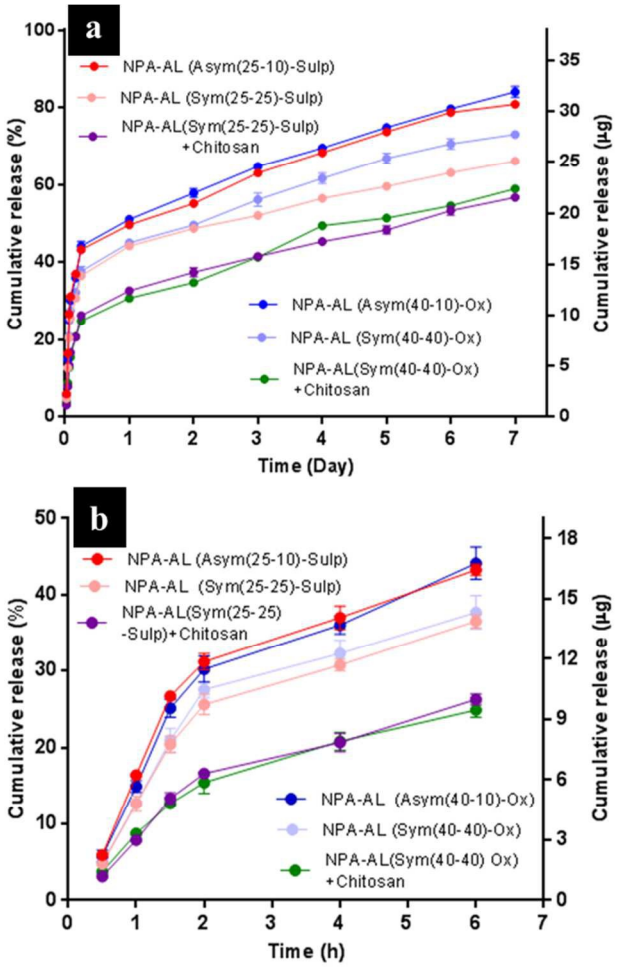

Fig. 8 *In vitro* drug release of indomethacin from various types of NPA-Al wire implant. Implants of small pore (NPA-$Al_{(Asym(25-10)-Sulp)}$), large pore (NPA-$Al_{(Sym(25-25)-Sulp)}$) and chitosan coated large pore (NPA-Al $_{(Sym(25-25)-Sulp)}$) from sulphuric acid group and small pore (NPA-Al $_{(Asym(40-10)-Ox)}$), large pore (NPA-$Al_{(Sym(40-40)-Ox)}$) and chitosan coated large pore (NPA-$Al_{(Sym(40-40)-Ox)}$) from oxalic acid group with a constant pore layer thickness of 20 µm were used in release studies in PBS for 7 days. Data represent means ± st.dev. from at least 3 samples.

Chitosan coated implants showed much lower burst drug release (i.e. only 22-25%) compared to the same types of implant without a coating (i.e. 32-34%). This coating also showed total reduced release of only 50-55% while uncoated implants exhibited 70-80% of the drug release. This indicates that chitosan can also be used to further extend and control the drug release from NPA-Al wire implants when necessary. This chitosan controlled release of drug supports our previous study on TNTs and NPA on flat substrates.[38]

Relative osteoblast cell attachment and spread ability with NPA-Al wire implants

An essential property of implant devices to be used in bone therapy is their biocompatibility and ability to interact with bone cells, especially with osteoblasts.[14,16] As a measure of this interaction, relative adhesion of osteoblasts to the NPA-Al wire implants, chitosan coated NPA-Al implants and control substrates of Al wire and cell culture plastic was performed. The total number of cells adherent to the surface of these substrates after different times of

attachment (3 and 6 h) was converted into a percentage of the total, and is graphically represented in Fig. 9.

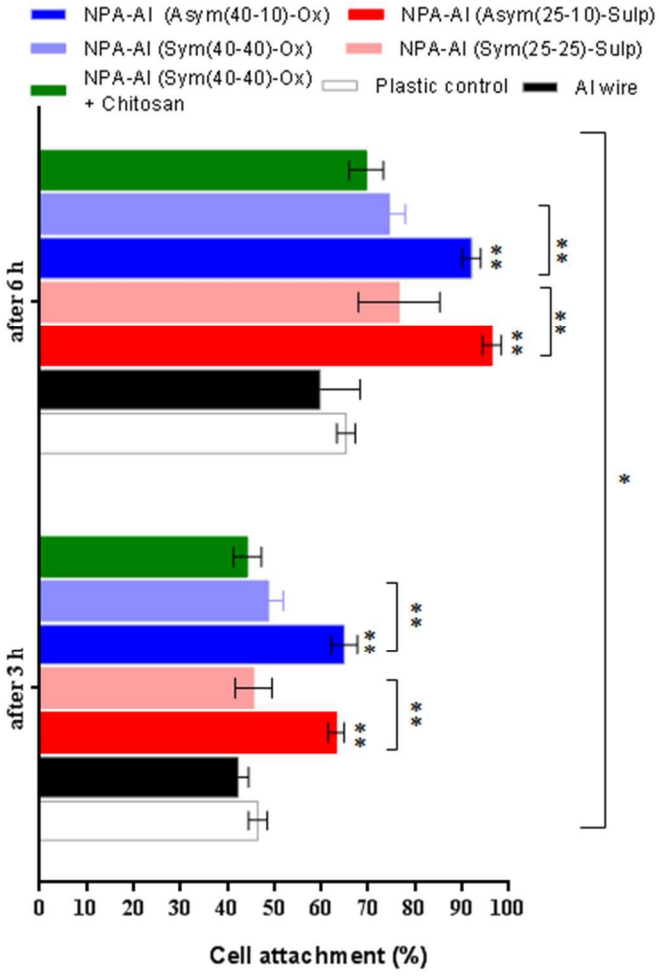

Fig. 9 Relative osteoblast cell attachment of NPA-Al wire implants after 3 and 6 h. Implants with multiple small pores (NPA-$Al_{(Asym(25-10)-Sulp)}$), large single pore (NPA-$Al_{(Sym(25-25)-Sulp)}$) and chitosan coated large single pore (NPA-Al $_{(Sym(25-25)-Sulp)}$) from sulphuric acid group and multiple small pores (NPA-Al $_{(Asym(40-10)-Ox)}$), large single pore (NPA-$Al_{(Sym(40-40)-Ox}$) and chitosan coated large single pore (NPA-$Al_{(Sym(40-40)-Ox)}$) from oxalic acid group, along with culture plastic and Al wire as controls were used. Cell attachment was investigated using a method that uses crystal violet. Data represent mean ± st.dev. from at least 3 samples. Asterisks denote significant difference to the plastic control (*$p < 0.01$, **$p < 0.001$).

The highest number of cells found adherent to substrate was taken as 100%. It was found that after 6 h of incubation all substrates showed significantly ($p< 0.01$) superior attachment of cells compared to their attachment measured after 3 h. This result is supported by our previous study on NPA-Al wire implants of 33 nm pore diameter, showing the spread and attachment of healthy osteoblast cells on to the implant surfaces.[35] After 3 h, implants {(NPA-$Al_{(Asym(25-10)-Sulp)}$ and (NPA-$Al_{(Asym(40-10)-Ox)}$}with a more porous structure and multiple small pores prepared either using sulphuric or oxalic acid showed significantly higher overall cell attachment compared to implants{(NPA-$Al_{(Sym(25-25)-Sulp)}$ and (NPA-$Al_{(Sym(40-40)-Ox)}$}with less porous structure with relatively large pore, chitosan coated implants and control substrates of cell culture plastic and Al wire. The more porous implants also showed significantly higher cell attachment compared to implants with a less porous structure, chitosan coated implants and control substrates after 6 h of incubation. NPA-$Al_{(Asym(25-10)-Sulp)}$ implants of multiple (3-6) small pores (10-14 nm diameter) in a single cell showed significantly different cell attachment compared to NPA-$Al_{(Sym(25-25)-Sulp)}$ implants with only a single large pore (25-30 nm diameter) in a cell, both fabricated using sulphuric acid. NPA-$AL_{(Asym(40-10)-Ox)}$ implants with multiple (5-7) small pores (7-10 nm diameter) in a single cell also showed significantly different cell attachment compared to NPA-$Al_{(Sym(40-40)-Ox)}$ implants containing only a single large pore (35 nm) in a cell, prepared using oxalic acid.

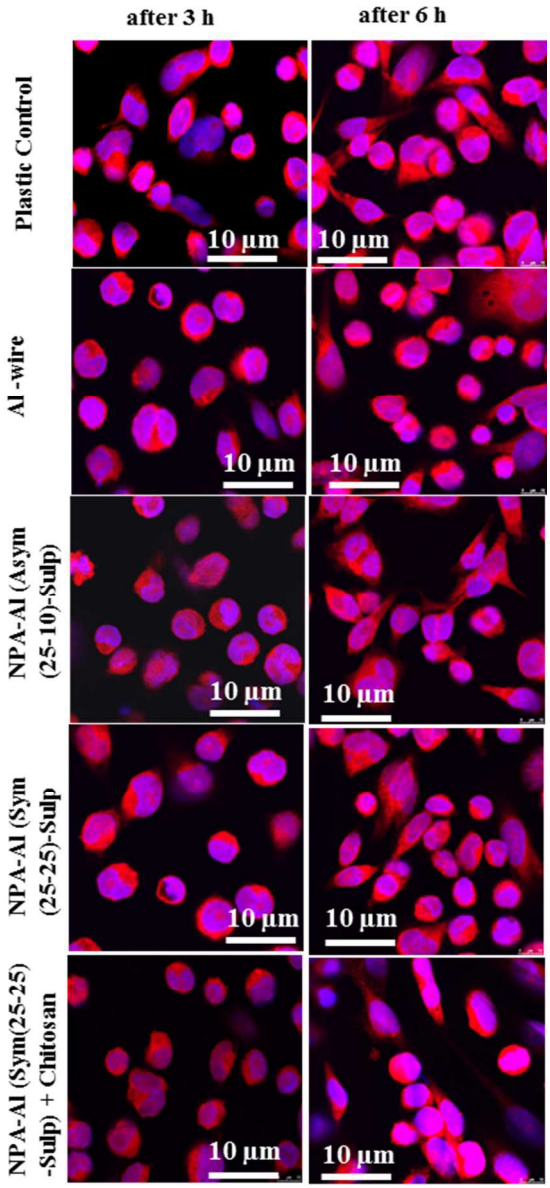

Fig. 10 Spreading of HOS osteoblast cells on NPA-Al wire implants after 3 and 6 h. imaged by confocal microscopy. Implants with multiple small pores (NPA-$Al_{(Asym(25-10)-Sulp)}$), large single pore (NPA-$Al_{(Sym(25-25)-Sulp)}$) and chitosan coated large single pore (NPA-Al $_{(Sym(25-25)-Sulp)}$) from sulphuric acid group and multiple small pores (NPA-Al $_{(Asym(40-10)-Ox)}$), large single pore (NPA-$Al_{(Sym(40-40)-Ox)}$) and chitosan coated large single pore (NPA-$Al_{(Sym(40-40)-Ox)}$) from oxalic acid group, along with culture plastic and Al wire as controls were used. Phalloidin (red, cytoskeleton) and DAPI (blue, nuclei) stains showed their clear spreading behaviour and interconnections between the cells in all cases. Images from oxalic acid group are not shown here due to the close similarity with the sulphuric acid group.

Surface modification of both NPA-Al$_{(Sym(25-25)-Sulp)}$ and NPA-Al$_{(Sym(40-40)-Ox)}$ implants using chitosan coating showed no enhanced effect in the cell attachment. Overall, these data indicate that NPA-Al wire implants with dense small pores and their resultant highly porous and rough surfaces promote osteoblast attachment. This finding is consistent with the general concept of the suitability of rough and porous biomaterials for enhanced bone cell growth and subsequent osseointegration.[44] Similar to this NPA on wire surfaces, NPA on a planar Al substrate with mixed pore structures have been reported to have a strong influence on cell attachment and cell–cell interaction.[46] Although it has been widely considered that large pores enhance the growth extension and protrusions of osteoblasts inside the large pore of NPA,[47] it appears that our finding is in direct contrast to the suitability of the large pore. However, it indirectly supports the fact as the dense and multiple small pores in this study increase the total surface area as well as porosity of the implants, therefore, enhanced attachment was observed due to the unique nanotopography of these implants. Furthermore, the cell adhesion data should be viewed in the context that tissue culture plastic is the gold-standard for cell attachment *in vitro*, and all NPA-Al substrates used were at least as effective as the control surface.

The ability of the cells to spread on different NPA-Al wire implants was observed using staining of the cells for cytoskeletal actin filaments using phalloidin (red) and for nuclei using DAPI (blue) after 3 and 6 h of incubation and their images collected using confocal microscopy are presented in Fig. 10. The images show that most of the cells are circular and intact after 3 h on all types of implant and the controls. However, cells showed evidence of spreading after 6 h of incubation. They also showed evidence of interconnectivity after that time, indicating that NPA-Al wire implants were able to support osteoblast attachment and viability. These results are in agreement with previous studies on NPA on planar surfaces showing that nanoporous anodized aluminium oxides give rise to biocompatible substrates and promote the growth of osteoblast cells.[16,48,49] The adhesion of cells to NPA surface also indicates that NPA-Al implants are favourable substrates for cells and are likely to promote the growth of bone tissue.

It is important to note here that highly stable chemistry of NPA doesn't allow release of structural impurities (such as carboxylates and sulphates) into the eluting medium under physiological conditions.[27,50,51] NPA layers on the wire surfaces are also strong enough to withstand insertion stress confirmed during *ex vivo* implantation into bone and shown in our previous study indicating their suitable mechanical properties for the proposed application.[35]

Conclusion

This work demonstrates that commercially available aluminium wires can be transformed into nanoengineered drug-releasing implants using simple a two-step electrochemical anodization process with oxalic and sulphuric acid. Our results confirmed that using both acids and a well-established standard anodization process conducted at constant voltage of 40 and 25 V can be adopted for scalable preparation of NPA-Al wire implants with different pore dimensions and altered nanopore topography. In particular, anodization using sulphuric acid has shown rapid and faster nanofabrication of NPA layers around Al wire implants similar to planar Al substrates. It was shown that the use of low anodization voltages of 10-15 V form controllable multiple small pores of 7-14 nm in a single cell of NPA, leading to highly porous NPA-Al wire implants. This study indicates that drug loading and release can be enhanced by increasing the number of pores and the surface area of the NPA-Al wire implants and their release can be further controlled using a thin biopolymer chitosan coating, which is widely used in bone applications. Our results showed that these biocompatible wire implants promote osteoblast cell attachment onto their surfaces and implants with a high density of very small pores or a highly porous structure have superior bone cell attachment ability. Compared with planar NPA substrates proposed for localized drug delivery applications, these variable forms of Al wire implants could be easily inserted into bone and used for direct delivery of therapeutics in bone. Considering the flexibility of using either oxalic or sulphuric acid electrolyte, the simple, low cost and scalable fabrication, controllable nanopore dimensions, and tuneable drug-releasing characteristics, these therapeutic NPA-Al wire implants appear to have considerable potential to address many limitations of systemic and other localized drug delivery systems. Their applications as drug-releasing implants for clinical applications to treat a range of bone diseases, including bone infection, bone inflammation, fracture management, bone healing and potentially for bone cancer are very promising.

Acknowledgments

The authors acknowledge the financial support of the Australian Research Council (FT110100711, DP 120101680 and DE140100549) and the University of Adelaide for this work. The support from the technical staff from the Adelaide Microscopy, University of Adelaide, for providing SEM and confocal imaging facilities is acknowledged.

Notes

[a] School of Chemical Engineering,
The University of Adelaide, SA 5005, Australia.
E-mail: dusan.losic@adelaide.edu.au (D. Losic)
[b] Centre for Orthopaedics and Trauma Research, School of Medicine
The University of Adelaide, SA 5005, Australia

References

1. P. J. Blackshear. *Sci. Am*, 1979, **241**, 66−73.
2. P. Wu, and D.W. Grainger. *Biomaterials*, 2006, **27**, 2450–2467.
3. D.W. Hutmacher. *Biomaterials*, 2000, **21**, 2529–2543.
4. R. Langer. *Science*, 2001, **293**, 58−59.
5. J.R. Porter, T.T. Ruckh and K.C. Popat. *Biotechnol Prog.*, 2009, **25**, 1539–1560.
6. H. Liu and T.J. Webster. *Biomaterials*, 2007, **28**, 354–369.
7. S. Rani, S.C. Roy, M. Paulose, O.K. Varghese, G.K. Mor, S. Kim, S. Yoriya, T.J. Latempa and C.A. Grimes. *Phys. Chem. Chem. Phys.*, 2010, **12**, 2780–2800.
8. D. Losic and S. Simovic. *Expert Opin. Drug Deliv.*, 2009, **6**, 1363–1381.
9. M. Colilla, M. Manzano and M.Vallet-Regi. *Int J Nanomed*., 2008, **3**, 403–414.
10. A.I. Pearce, R.G. Richards, S. Milz, E. Schneider and S.G. Pearce. *Eur. Cell. Mater.*, 2007, **13**, 1–10.
11. P. Roy, S. Berger and P. Schmuki. *Angew Chem Int Ed Engl.*, 2011, 50, 2904–2939.
12. A. Ghicov and P. Schmuki. *Chem. Commun.* (Camb), 2009, **2**, 2791–2808.
13. S. Bauer, P. Schmuki, V.D.M Klaus and P. Jung. *Prog. Mater. Sci.*, 2013, **58**, 261–326.
14. A. Santos, M. S. Aw, M. Bariana, T. Kumeria, Y. Wang and D. Losic. *J. Mater. Chem. B*, 2014, **2**, 6157–682.
15. K. Gulati, M.S. Aw and D. Losic. *Int. J. Nanomed.*, 2012, **7**, 2069–2076.

16. D. Losic, M.S. Aw, A. Santos, K. Gulati, and M. Bariana. Expert Opin. Drug Deliv., 2015, **12**,103–127.
17. M.S. Aw, K.A. Khalid, K. Gulati, G.J. Atkins, P. Pivonka, D.M. Findlay and D. Losic. *Int. J. Nanomed*., 2012, **7**, 4883–4892.
18. L. Sedel. *Clin. Orthopaed. Relat. Res.*, 2000, **379**, 48–54.
19. A.M. Md Jani, D. Losic and N.H. Voelcker. *Prog. Mater. Sci.*, 2013, **58**, 636–704.
20. K.C. Popat, K.I. Chatvanichkul , G.L. Barnes , T.J. Latempa , C.A. Grimes and T.A. Desai. *J. Biomed. Mater. Res. Part A*, 2007, **80**, 955–964.
21. E.E.L. Swan, K.C. Popat and T.A. Desai. *Biomaterials*, 2005, **26**, 1969–1976.
22. K.C. Popat, E.E. Leary Swan, V. Mukhatyar, K.I. Chatvanichkul, G.K. Mor, C.A. Grimes and T.A. Desai. *Biomaterials*, 2005, **26**, 4516–4522.
23. E.E. Swan, K.C. Popat, C.A. Grimes and T.A. Desai. *J. Biomed. Mater. Res. Part A*, 2005, **72**, 288–295.
24. M. Karlsson, E. Palsgard, P.R.Wilshaw and L.D. Silvio. *Biomaterials*, 2003, **24**, 3039–3046.
25. J. J. Klawitter, A.M. Weinstein, F.W. Cooke, L.J. Peterson, B. M. Pennel and R.V. McKinney. *J. Dental. Res.*, 1977, **56**, 768–776.
26. M. Mour, D. Das, T. Winkler, E. Hoenig, G. Mielke, M.M. Morlock, and A.F. Schilling. *Materials*, 2010, **3**, 2947–2974.
27. J.J. Wykrzykowska, Y. Onuma and P.W. Serruys. *Expert Opin. Drug Deliv.*, 2009, **6**, 113–126.
28. H. Wieneke, O. Dirsch, T. Sawitowski, Y.L. Gu, H. Brauer, U. Dahmen, A. Fischer, S. Wnendt, and R. Erbel. *Catheterizat. Cardiovasc. Intervent.*, 2003, **60**, 399–407.
29. H.J. Kang, D.J. Kim, S.J. Park, J.B.Yoo, and Y.S. Ryu. *Thin Solid Films*, 2007, **515**, 5184–5187.
27. K.E. L. Flamme, K.C. Popat, L. Leonic, E. Markiewiczc, T.J. La Tempad, B.B. Romanc, C.A. Grimesd and T.A. Desai. *Biomaterials*, 2007, **28**, 2638–2645.
28. C.M. Davies, D.B. Jones, M.J. Stoddart, K. Koller, E. Smith, C.W. Archer and R.G. Richards. *Eur. Cell. Mater*., 2006,**11**, 57–75.
29. K. Gulati, M.S. Aw and D. Losic. *Nanoscale Res. Lett.*, 2011, **6**, 571–576.
30. H. Masuda and K. Fukuda, *Science*, 1995, 268, 1466−1468.
31. H. Masuda and F. J. Hasegwa. *Electrochem. Soc*., 1997, **144**, L127−L130
32. J.M. Montero-Moreno, M. Sarret and C. Müller. *J. Electrochem. Society*, 2007, **154**, C169–C174.
33. Ho, AYY; H Gao, YC Lam, I.Rodríguez, *Adv. Func. Mater.*, 2008, **18**, 2057–2063.
34. A. Santos, J. Ferré-Borrull, J. Pallarès and L.F. Marsal. *Physica Status Solidi a*, 2011, **208**, 668–674.
35. S. Rahman, G.J. Atkins, D.M. Findlay and D. Losic. *J. Mater. Chem. B*, 2015, **3**, 3288–3296.
36. T. Kumeria, A. Santos and D. Losic. *Sensors*, 2014, 14, 11878–11918.
37. C.S. Law, A. Santos, T. Kumeria and D. Losic. *ACS Appl. Mater. Interface*, 2015, 7, 3846–3850.
38. K. Gulati, S. Ramakrishnan, M. Sinn Aw, G.J. Atkins, D.M. Findlay, and D. Losic. *Acta Biomaterialia*, 2012, **8**, 449–456.
39. G.J. Atkins, S. Bouralexis, A. Evdokiou, S. Hay, A. Labrinidis, A.C. Zannettino, D.R. Haynes and D.M. Findlay. *Bone*, 2002, **31**, 448–456.
40. U.W. Jung, K.Y. Song, C.S. Kim, Y.K. Lee, K.S. Cho, C.K. Kim and S.H. Choi. *Biomed. Mater.*, 2007, **2**, S101–105.
41. W. Lee, R. Ji, U. Gösele and K. Nielsch, *Nat. Mater.*, 2006, **5**, 741–747.
42. K. Nielsch, J. Choi, K. Schwirn, R. B. Wehspohn and U. Gösele. *Nano Lett.*, 2002, **2**, 677–680.
43. O. Jessensky, F. Müller and U. Gösele. *Appl. Phys. Lett.*, 1998, **72**, 1173–1175.
44. W. Lee and J. S. Park. *Chem. Rev.*, 2014, **114**, 7487–7556.
45. D. Losic, L. Velleman, K. Kant, T. Kumeria, K. Gulati, J.G. Shapter, D. A. Beattie, S. Simovic, *Australian J. Chem.*, 2011,**64**, 294–301.
46. K. Kant, S.P. Low, A. Marshal, J.G.Shapter and D. Losic. *ACS Appl. Mater. Interface*, 2010, **2**, 3447–3454.
47.M. Karlsson and L. Tang. *J Mater Sci: Mater. Med.*, 2006, **17**,1101–1111.
48. S. Simovic, D. Losic and K. Vasilev. *Chem. Commun.*, 2010, **46**, 1317–1319.
49. K. Anselme, L. Ploux, A. Ponche and J. Adhes. *Sci. Technol.*, 2010, **24**, 831–852.
50. A. Santos, M. Alba, M. Rahman, P. Formentín, J. Ferré-Borrull, J. Pallarès and L.F Marsal. *Nanoscale Res. Lett.*, 2012, **7**, 228–238
51. Y. Wang, A. Santos, G. Kaur, A. Evdokiou and D. Losic. *Biomaterials*, 2014, **35**, 5517